AIAA JOURNAL
Vol. 32, No. 4, April 1994

Turbulence Models for Compressible Boundary Layers

P. G. Huang*
Eloret Institute, Palo Alto, California 94303
P. Bradshaw†
Stanford University, Stanford, California 94305
and
T. J. Coakley‡
NASA Ames Research Center, Moffett Field, California 94035

It is shown that to satisfy the generally accepted compressible law of the wall derived from the Van Driest transformation, turbulence modeling coefficients must actually be functions of density gradients. The transformed velocity profiles obtained by using standard turbulence model constants have too small a value of the effective von Kármán constant κ in the log-law region (inner layer). Thus, if the model is otherwise accurate, the wake component is overpredicted and the predicted skin friction is lower than the expected value. The magnitude of the errors that result from neglecting this dependence on density depends on the variable used to specify the length scale. It will be shown that the k-ω model is less dependent on density gradient than the k-ε model, although it is not completely free from errors associated with density terms. We propose models designed to reduce the density-gradient effect to an insignificant level. To agree with experimental values for κ in compressible boundary layers, the apparent eddy viscosity must be increased. This compressibility effect—which is an artifact of conventional turbulence modeling rather than something real—is exactly opposite to that in mixing layers. There the growth rate, and by implication the eddy viscosity, decreases with increasing Mach number: since the growth rate of low-speed mixing layers is not much affected by mean density differences across the layers, the Mach-number effect is a real compressibility effect. However, it first appears at turbulence Mach numbers above those found in nonhypersonic boundary layers. As a consequence, recent compressibility modifications proposed for the mixing layer are liable to increase the errors in predictions of flat-plate compressible boundary layer flows.

I. Introduction

CALCULATIONS of high Mach number turbulent flows have become a major challenge in computational fluid dynamics in recent years. Traditionally, models developed originally for incompressible flows have been applied to compressible flows with little or no modification when mass-weighted (Favre) dependent variables are employed. Our investigation centers on the dissipation-transport equation and its role in predicting the compressible law of the wall. This equation, or some other equation implying a length scale for the turbulence, is used not only in two-equation eddy-viscosity-transport models but also in full Reynolds-stress transport models. Therefore, although the discussion that follows centers on two-equation models, for simplicity, the results apply at least qualitatively to full Reynolds-stress transport models, which, like two-equation models, usually reduce to local energy equilibrium in the wall layer.

The Van Driest compressible law of the wall is derived from inner-layer similarity arguments, leading to the mixing-length formulas for velocity and temperature[1,2]

$$\frac{\partial U}{\partial y} = (\tau_w/\rho)^{1/2}/\kappa y \tag{1}$$

$$\frac{\partial T}{\partial y} = -q/[\rho c_\pi(\tau_w/\rho)^{1/2}\kappa_T y] \tag{2}$$

where $q = q_w + U\tau_w$. Assuming that $\tau = \tau_w$ and that κ and κ_T are constants, integration of Eqs. (1) and (2) yields the velocity and temperature profiles as:

$$U_c^+ = U_c/u_\tau = \frac{1}{\kappa}\ell_n y^+ + C \tag{3}$$

$$T = T_w - Pr_t U q_w/(c_p\tau_w) - Pr_t U^2/(2c_p) \tag{4}$$

where $Pr_t \equiv \kappa/\kappa_T$, being the wall-layer value of the turbulent Prandtl number, u_τ and y^+ are defined with respect to the physical properties at the wall, as

$$u_\tau = (\tau_w/\rho_w)^{1/2} \tag{5}$$

and

$$y^+ = yu_\tau/\nu_w \tag{6}$$

Finally, the Van Driest transformed velocity U_c is defined by

$$U_c = \int_0^U \left(\frac{\rho}{\rho_w}\right)^{1/2} dU \tag{7}$$

Substituting Eq. (4), with $\rho/\rho_w = T_w/T$, into Eq. (7) yields

$$U_c = E^{1/2}\left[\sin^{-1}\left(\frac{A+U}{D}\right) - \sin^{-1}\left(\frac{A}{D}\right)\right] \tag{8}$$

where $E = 2c_pT_w/Pr_t$, $A = q_w/\tau_w$, and $D = (A^2 + E)^{1/2}$.

Received April 5, 1993; revision received Aug. 25, 1993; accepted for publication Aug. 26, 1993.

*Research Scientist; mailing address: NASA Ames Research Center, MS 229-1, Moffett Field, CA 94035. Senior Member AIAA.

†Thomas V. Jones Professor, Department of Mechanical Engineering. Member AIAA.

‡Research Scientist, Modeling and Experimental Validation Branch. Associate Fellow AIAA.

Fernholz and Finley[3] have reviewed a wide range of high-Mach-number boundary layer data and shown that most of the data collapse onto the Van Driest compressible law of the wall, using $\kappa = 0.4$ and $C = 5.1$, even though in principle the constants of integration in Eqs. (3) and (4) can be functions of the friction Mach number $u_\tau/c_w \equiv u_\tau/\sqrt{(\gamma-1)c_pT_w}$ where c is the speed of sound, and the dimensionless heat-transfer parameter $B_q = q_w/(\rho_w c_p u_\tau T_w)$. Recently, Huang et al.[4] extended Eq. (3) to include the viscous wall region and the wake. The velocity profile family has been shown to represent experimental zero-pressure-gradient boundary layer velocity profiles accurately over a wide range of Mach numbers and Reynolds numbers. In addition, the skin friction obtained based on the velocity profile family was compared with experimental data and again the results were very good. The constants used by Huang et al. were $\kappa = 0.41$, $C = 5.2$, and $Pr_t = 0.9$. The log-law slope $1/\kappa$ is difficult to evaluate from fits to experimental data: the nearest to a canonical value is that obtained by Coles[5] in an extensive survey of low-speed boundary layers, $\kappa = 0.41$. Obviously an increase in best-fit κ implies an increase in C, and different choices of log-law constants are best compared by evaluating U/u_τ somewhere in the middle of the log-law region, say $y^+ = 100$ for laboratory measurements. Fernholz and Finley's constants give $U/u_\tau = 16.61$, ours 16.43—a difference of only 1%, which is negligible.

Equation (3), plotted in Fig. 1, represents the present consensus to which turbulence models should be matched: it is based on exhaustive data surveys,[3,4] so in the interest of clarity we have not included any data in Fig. 1. The purpose of this paper is to compare this equation with results from calculations of compressible turbulent boundary layer flows using standard turbulence models.[6-8] These results are for high-Reynolds-number versions of the turbulence models coupled with compressible-wall-function treatments,[9] although similar behavior has been observed in results obtained by integrating low-Reynolds-number models from $y = 0$. Because the concern is with behavior in the log-law region the treatment of the viscous wall region is not an issue: it can change C in Eq. (3) but not κ.

Figure 1 shows calculations of an adiabatic wall at $M_e = 5$ by three different models, with a baseline calculation at $M_e = 0.1$ using the k-ε model. (The standard model coefficients are $c_\mu = 0{,}09$, $c_{e1} = 1.44$, $c_{e2} = 1.92$, $\sigma_k = 1$, and $\sigma_\varepsilon = 1.3$. However, in this paper, the value of σ_ε is altered from 1.3 to 1.17 to give a better fit to the incompressible law of the wall [see discussion after Eq. (14)]). At low Mach numbers the profile predicted by the k-ε model follows the law of the wall, Eq. (3), very well up to $y^+ \approx 500$ and, although not shown here, the wake profile correctly matches the law of the wake of Coles.[5]

The bulk Reynolds number should not affect the law of the wall, but for uniformity we have done our high-Mach-number calculation at the same Reynolds number $y_\delta^+ = u_\tau\delta/\nu_w$ as the $M_e = 0.1$ calculation. This seemed a better choice for law-of-the-wall comparisons than constant Re_θ: in low-speed flow, $y_\delta^+ \approx 3{,}500$ at $Re_\theta = 10{,}000$, while for air flow at $M_e = 5$ over an insulated surface this value of y_δ^+ corresponds to $Re_\theta = 46{,}000$. As shown in Fig. 1, the k-ε model calculation at $M_e = 5$ displays an early rise of the profile above the transformed log law, and hence results in a wake component (maximum derivation of profile from standard log law, $\Delta U_c^+ \equiv 2\Pi/\kappa$) twice the low-speed value. This large value of wake component is not supported by the experimental data assembled by Fernholz and Finley[3]: they concluded that the wake parameter Π is nearly the same function of their empirically chosen Reynolds number as at low speed and therefore about 0.58 in our Reynolds number range. An overly large wake component implies an underestimate of skin friction. It should be noted that the excessively large wake predicted by the k-ε model is also observed in the profile obtained from the Reynolds stress transport model (RSTM) of Gibson and Launder.[10] In contrast, the profile calculated using the k-ω model of Wilcox[11] shows only a small increase of the slope in the log-law region. The preceding results clearly indicate that standard turbulence models do not accurately predict boundary layers at high Mach number, and since the error is worst in the k-ε and Reynolds-stress transport models it appears that the trouble lies in the ε equation, which is used in these models but not in the k-ω model.

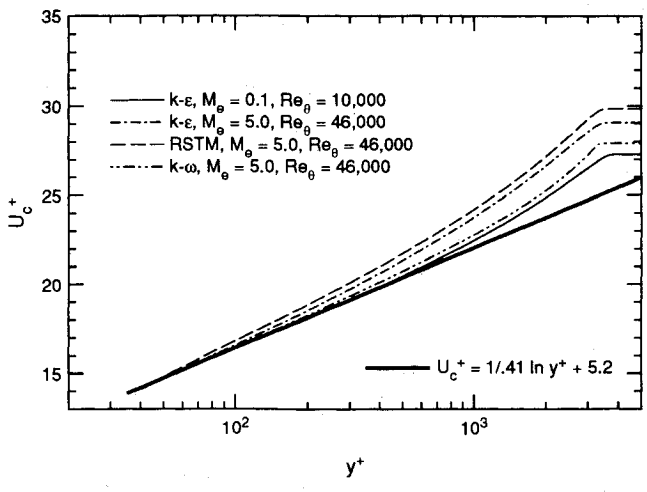

Fig. 1 Transformed velocity profiles obtained by k-ε, k-ω, and RSTM models with compressible wall functions; adiabatic wall calculations.

II. Assessment of Closure Coefficients

In this section, we discuss only the extension of incompressible turbulence models using Favre density-weighted averaging. It is important to realize that the discrepancies discussed in the present paper are attributable to mean density gradient, not density fluctuations. They are an order of magnitude larger than differences between Favre averaging and conventional averaging. In this section, additional compressibility terms are assumed unimportant and we shall discuss effects of these modeled terms in Sec. IV. Attention is also focused on the inner layer of a constant-pressure boundary layer, where the results can be compared with the transformed log law and where convective transport can be neglected to simplify the governing equations to ordinary differential ones in y, sometimes called the Couette flow analysis. If the eddy-viscosity hypothesis is formally applied, the velocity profile in the constant-stress inner layer is governed by

$$\frac{d}{dy}\left(\mu_t \frac{dU}{dy}\right) = 0 \tag{9}$$

where μ_t is the eddy viscosity. For the k-ε two-equation model, we write $\mu_t = c_\mu \rho k^2/\varepsilon$ in which the dimensionless coefficient c_μ is fixed at 0.09 to satisfy $-\overline{uv}/k = 0.3$ in local equilibrium.

As we shall see later, the difficulties seem to be associated with the length-scale equation for ε or ω, and we therefore define a general variable ϕ in terms of ε:

$$\phi = \rho^n k^m \varepsilon^l \tag{10}$$

Equation (10) allows construction of a variety of length-scale variables by assigning different values to n, m, and l: for example $n = 0$, $m = -1$, and $l = 1$ gives $\phi \equiv \omega = \varepsilon/k$.

The standard transport equations for k and ϕ, in the Couette-flow approximation, will be assumed to be in the form;

$$-\frac{d}{dy}\left(\frac{\mu_t}{\sigma_k}\frac{dk}{dy}\right) = \rho P_k - \rho\varepsilon \tag{11}$$

and

$$-\frac{d}{dy}\left(\frac{\mu_t}{\sigma_\phi}\frac{d\phi}{dy}\right) = c_1 \rho P_k \frac{\phi}{k} - c_2 \rho \varepsilon \frac{\phi}{k} \tag{12}$$

where σ_k and σ_ϕ are turbulent Prandtl numbers for k and ϕ, respectively, and P_k is the turbulent-kinetic energy production

$$P_k = -\overline{uv}\frac{dU}{dy} = \nu_t\left(\frac{dU}{dy}\right)^2 \tag{13}$$

where $-\overline{uv} = \tau/\rho = \tau_w/\rho$.

In Eq. (12), c_1 and c_2 are dimensionless coefficients, related to the corresponding coefficients of the ε equation, $c_{\varepsilon 1}$ and $c_{\varepsilon 2}$, by

$$\begin{aligned} c_1 &= lc_{\varepsilon 1} + m \\ c_2 &= lc_{\varepsilon 2} + m \end{aligned} \tag{14}$$

In the standard k-ε model, $c_{\varepsilon 2} = 1.92$, while in the newer two-equation models, such as the k-ω models, c_2 is adjusted to give $c_{\varepsilon 2} = 1.83$ to provide a better fit of the decay law of homogeneous isotropic turbulence.[11] The value of $c_{\varepsilon 1}$ is generally determined by computer optimization and is 1.44 and 1.56 for the k-ε and the k-ω models, respectively. The value of σ_ϕ is chosen to satisfy the incompressible law of the wall; $\sigma_\phi = 1.17$ and 2 for the k-ε and the k-ω models, respectively. [The value of σ_ϕ is defined from Eq. (15) with RHS = 1 and $\kappa = 0.41$.] Finally, σ_k is fixed to optimize prediction of the turbulent kinetic energy profile across the boundary layer; $\sigma_k = 1$ and 2 for the k-ε and the k-ω models, respectively.

To ensure that the plot of U_c^+ against $\ell_n y^+$ has a slope of $1/\kappa$ in the logarithmic region, a unique relation must exist between κ and the other coefficients. The derivation of this relation is similar to that for the incompressible case, but with the following density effects taken into account. First, in this region $dk/dy = 0$ is replaced by $d\rho k/dy = 0$, because $-\overline{\rho u v}/k$ = constant and $\tau = \tau_w = -\rho\overline{uv}$. It should be noted that in low-speed constant-pressure flow $dk/dy = 0$ in the inner layer and σ_k is immaterial. Although we include the diffusion of k for completeness in this study, it will be seen later that its effect is very small. Second, the dissipation relation $\varepsilon = u_\tau^3/\kappa y$ is replaced by $\varepsilon = (\tau_w/\rho)^{3/2}/\kappa y$. Finally, the density can no longer be factored out of the diffusion terms, $d/dy\,(\mu_t \ldots) \neq (1/\rho)\, d/dy\,(\nu_t \ldots)$.

By substituting the above-mentioned assumptions into Eq. (12), we obtain

$$\frac{c_\mu^{1/2}\sigma_\phi}{l^2\kappa^2}(c_2 - c_1) = 1 + \frac{1}{l^2} \times \left[d_1 \frac{y}{\rho}\frac{d\rho}{dy} + d_2 \frac{y^2}{\rho}\frac{d^2\rho}{dy^2} + d_3\left(\frac{y}{\rho}\frac{d\rho}{dy}\right)^2 \right] \tag{15}$$

where

$$\begin{aligned} d_1 &= n - m - 2l + 3l^2 + 2ml - 2nl + c_1\frac{\sigma_\phi}{\sigma_k} \\ d_2 &= n - m - \frac{3}{2}l + c_1\frac{\sigma_\phi}{\sigma_k} \\ d_3 &= \left(n - m - \frac{3}{2}l\right)\left(n - m - \frac{3}{2}l - \frac{1}{2}\right) - \frac{3}{2}c_1\frac{\sigma_\phi}{\sigma_k} \end{aligned} \tag{16}$$

It can be seen that to extend the models for incompressible flows to compressible flows, recovering Eq. (1) without having to adjust the closure coefficients on the left-hand side of Eq. (15), the second term on the right-hand side of Eq. (15) must be negligible compared to unity.

Table 1 lists the coefficients d_1 to d_3 for the k-ε and k-ω models. Assuming that pressure is independent of y in the boundary-layer approximation, the density gradient can be related to the temperature gradient as

$$\frac{1}{\rho}\frac{d\rho}{dy} = -\frac{1}{T}\frac{dT}{dy} \tag{17}$$

Table 1 Coefficients associated with density-gradient terms

Model	n	m	l	d_1/l^2	d_2/l^2	d_3/l^2
k-ε	0	0	1	2.68	0.18	0.48
k-ω	0	−1	1	0.56	0.06	−0.33

where the temperature gradient dT/dy can be obtained by using Eqs. (1) and (2). By substituting Eqs. (17), (1), (2), and (4) into Eq. (15) and using Eq. (8) to relate U to the transformed velocity U_c for a given gas, one may express the right-hand side of Eq. (15) in terms of only three dimensionless groups, $M_\tau = u_\tau/c_w$, $B_q = q_w/(\rho_w c_p u_\tau T_w)$, and U_c^+, so that

$$\frac{c_\mu^{1/2}\sigma_\phi}{l^2\kappa^2}(c_2 - c_1) = 1 + \left(\frac{d_1 - d_2}{\kappa l^2}\right)S + \left(\frac{3/2\,d_2 + d_3}{\kappa^2 l^2}\right)S^2 + \frac{d_2}{l^2}\frac{Pr_t(\gamma - 1)M_\tau^2}{\kappa^2} \tag{18}$$

where

$$S = \frac{\sqrt{2Pr_t(\gamma - 1)}\,M_\tau \sin(s) + Pr_t B_q \cos(s)}{\cos(s) - \dfrac{B_q}{M_\tau}\sqrt{\dfrac{Pr_t}{2(\gamma - 1)}}\sin(s)} \tag{19}$$

and $s = \sqrt{Pr_t(\gamma - 1)/2}\,M_\tau U_c^+$.

By substituting d_1 to d_3 in Table 1 into the right-hand side of Eq. (18), for the k-ε model and the k-ω model, respectively, one obtains for the right-hand side of Eq. (18):

$$\begin{aligned} &1 + 6.10\,S + 4.46\,S^2 + 0.39\,M_\tau^2 \qquad (k\text{-}\varepsilon \text{ model}) \\ &1 + 1.22\,S - 1.49\,S^2 + 0.12\,M_\tau^2 \qquad (k\text{-}\omega \text{ model}) \end{aligned} \tag{20}$$

As may be seen from Eq. (20), the coefficients of the k-ω model are smaller than those of the k-ε model, so that the latter deviates less from the Van Driest compressible law of the wall (Fig.1).

It should be noted that the last terms involving $c_1(\sigma_\phi/\sigma_k)$ on each line of Eq. (16) come from the diffusion of k ($\partial\rho k/\partial y = 0$ instead of $\partial k/\partial y = 0$) and are of the same order as the other terms. However their net effect in Eq. (15) is small due to the cancellation of the terms, as can be seen from Eq. (18) where the only relevant term due to the k diffusion is $c_1(\sigma_\phi/\sigma_k)Pr_t(\gamma - 1)M_\tau^2/(l\kappa)^2$—a small quantity, because as will be seen later, M_τ is generally small. The other terms not involving $c_1(\sigma_\phi/\sigma_k)$ on each line of Eq. (16) come from the diffusion of φ, and do not necessarily cancel. Thus, we conclude that the choice of the variable φ is the main cause of the discrepancies between current turbulence model prediction and the Van Driest law of the wall.

Wilcox[12] solved the Couette flow equations analytically and provided the following approximate solutions, for the k-ε and k-ω models, respectively:

$$\begin{aligned} U_c^+ &\approx \frac{1}{K}\ell_n y^+ + \frac{1}{K}\ell_n\left(\frac{\rho}{\rho_w}\right)^{5/4} + \text{const} \quad (k\text{-}\varepsilon \text{ model}) \\ U_c^+ &\approx \frac{1}{K}\ell_n y^+ + \frac{1}{K}\ell_n\left(\frac{\rho}{\rho_w}\right)^{1/4} + \text{const} \quad (k\text{-}\omega \text{ model}) \end{aligned} \tag{21}$$

where $K = \sigma_\phi^{1/2}(c_2 c_\mu \Gamma - c_1/\Gamma)^{1/2}$ and Γ can be shown to have the following form:

$$\Gamma = \frac{\sqrt{M_\tau^4 Pr_t^2(\gamma - 1)^2 + 4c_\mu\sigma_k^2} - M_\tau^2 Pr_t(\gamma - 1)}{2c_\mu\sigma_k} \tag{22}$$

The density ratio in Eq. (21) can be obtained from Eq. (4) and shown to have the following form:

$$\frac{\rho}{\rho_w} = \frac{T_w}{T} = \frac{1}{\left[\cos(s) - \dfrac{B_q}{M_\tau}\sqrt{\dfrac{Pr_t}{2(\gamma - 1)}}\sin(s)\right]^2} \tag{23}$$

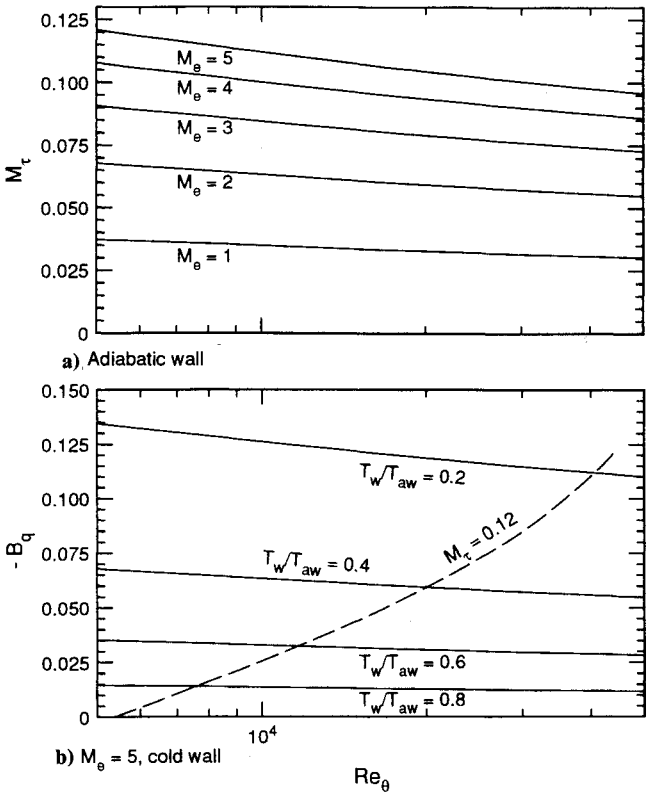

Fig. 2 Variation of M_τ and B_q under different conditions: a) adiabatic wall and b) cooled wall, $M_e = 5$.

It should be noted that K in Eq. (21) is not an effective von Kármán constant, because the additional term resulting from the density ratio ρ/ρ_w also contributes to the slope of the velocity profile. One can see from Eqs. (21–23) that the effective κ is a function of M_τ, B_q, and U_c^+ (or y^+), which is in accordance with the analysis shown in Eq. (18). Although Wilcox's analysis does not explicitly show how the velocity profile is altered by the density effects, it indicates that the density-related terms in the k-ε model have a stronger impact on κ than does the k-ω model, because the exponent of (ρ/ρ_w) is 5/4 for the k-ε model as compared to 1/4 for the k-ω model.

To estimate the error caused by the models, we have solved the Couette flow equations (9), (11), and (12) by a finite difference method. The temperature profile is given by Eq. (4). The solution of these equations requires boundary conditions at two end points. However, the inner layer profiles are functions of only M_τ, B_q, and y^+ for a given gas, and the solution is strictly independent of the outer boundary conditions. In the actual calculations, we have simply used Eq. (3) as the inner boundary condition at an arbitrary y^+ of 30. We have taken an arbitrarily large local Mach number at the outer boundary (say, $M_e = 30$), so that the value of y_δ^+ is calculated iteratively by the shooting method. Finally, boundary values of k and ϕ are calculated from $k = (\tau_w/\rho)/c_\mu^{1/2}$ and $\phi = (\rho^{n-3l/2-m}\tau_w^{3l/2+m}/c_\mu^{m/2})/(\kappa y)^l$.

The results below are reported for given values of M_τ and B_q. Figure 2 shows typical values of these quantities for air in terms of the more familiar bulk parameters, M_e and T_w/T_{aw}, over a range of Reynolds numbers Re_θ. These results were obtained using the velocity profile family illustrated in Huang et al.[4] For adiabatic wall conditions corresponding to the results shown in Fig. 3, we fixed $B_q = 0$ and varied M_τ from 0.06 to 0.12, representing a Mach 2–5 air flow over an insulated surface at $Re_\theta \approx 10{,}000$. For air flow over a cold wall as in the calculations shown in Fig. 4, we have fixed $M_\tau = 0.12$ and varied B_q from 0 to −0.12, corresponding to the conditions shown as the dashed line in Fig. 2b.

Figure 3 shows comparisons of the k-ε and the k-ω models for $B_q = 0$ and M_τ ranging from 0.06 to 0.12. As can be seen from the figure, the k-ε model is very sensitive to M_τ, causing the transformed velocity to rise as M_τ increases. On the other hand, the k-ω solutions are less dependent on M_τ.

For the cold wall cases, Fig. 4 shows the comparison of the k-ε and the k-ω models for $M_\tau = 0.12$ and B_q ranging from 0 to −0.12. Again, the results show that the k-ε model is more sensitive to the variations of B_q than the k-ω model: with increasing heat transfer to the wall, the profile predicted by either model moves closer to the compressible law of the wall.

III. Possible Remedies

One obvious way to predict the correct Van Driest law-of-the-wall profile is to incorporate the density-gradient terms directly into the coefficient c_1 defined in Eq. (14) using an iterative procedure to force the k-ε model to reproduce the expected law-of-the-wall profile. We chose to adjust c_1 rather than σ_ϕ because the analysis leading to Eq. (15) is tractable only under the assumption that sf is a constant. However, the gradient diffusion term is clearly the culprit. However, as shown in Fig. 5, the value of c_1 required in the ε-equation for $M_\tau = 0.12$ and $B_q = 0$ drops to 50% of its original value, $c_{1,0}$, at $y^+ = 1000$. This is too drastic a change to be acceptable.

Another possible remedy is to find a new model which will make d_1, d_2, and d_3 all zero. Unfortunately, substituting Eq. (14) into Eq. (16) gives the solution $n = m = l = 0$. Since this is not meaningful, it seems best to choose a model which will allow two leading coefficients, such as d_1 and d_2, to equal zero. Assuming $n = 0$ and $m = -1$, the solution $l = 5/6$ and $c_1(\sigma_\phi/\sigma_k) = 0.25$, implying a k-$\varepsilon^{5/6}/k$ model, makes both d_1 and d_2 equal to zero. On the other hand, if one assumes $n = 0$ and $m = -l$, the requirement for d_1 and d_2 to equal zero will lead to a $k-(\varepsilon/k)^{1/2}$ (or, $k-\sqrt{\omega}$) model. These two models give rise to an additional constraint on the relation between σ_κ and σ_ϕ because $c_1(\sigma_\phi/\sigma_k)$ is a known value obtainable from the solution satisfying d_1 and d_2 equal to zero. Calculations have demonstrated that these models do indeed reduce the density effects to insignificant levels; the difference between the predicted transformed velocity and the theoretical one at $y^+ = 1000$ is equal to 0.43 and 0.15% for the $k-\sqrt{\omega}$ and the k-$\varepsilon^{5/6}/k$ models, respectively. However, when applying these two models in the calculations employing compressible wall functions, we have found that

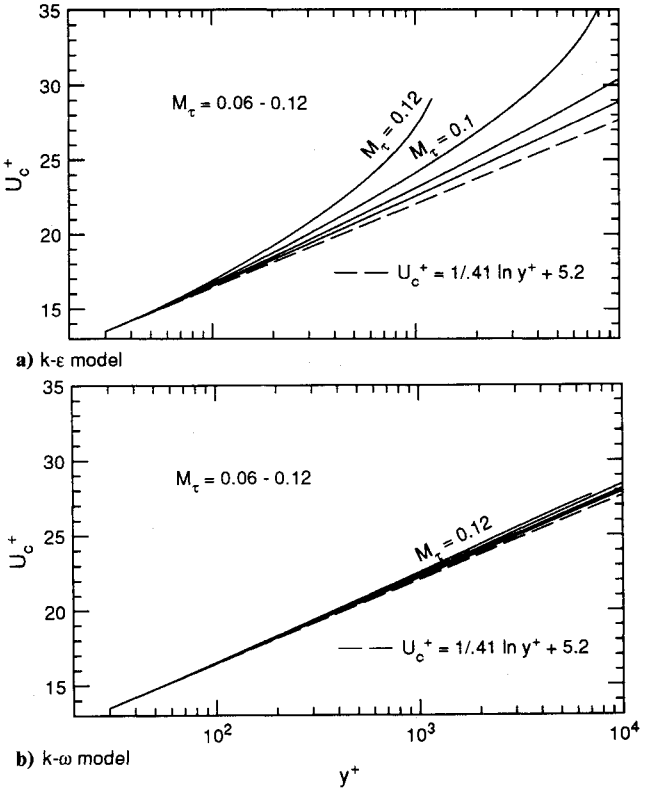

Fig. 3 Comparison of the k-ε and k-ω models in predicting the compressible law of the wall for an adiabatic wall ($B_q = 0$); M_τ ranges from 0.06 to 0.12 at an interval of 0.02: a) k-ε model and b) k-ω model.

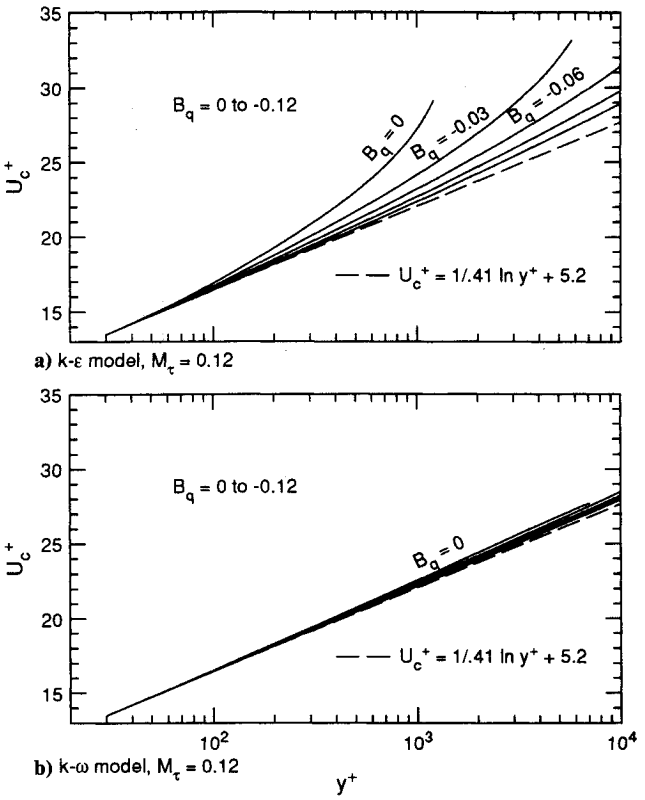

Fig. 4 Comparison of the k-ε and k-ω models in predicting the compressible law of the wall for a cold wall; M_τ = 0.12 and B_q ranges from 0 to −0.12 at an interval of −0.03: a) k-ε model and b) k-ω model.

the models are sensitive to the freestream values of the new variables, $\sqrt{\omega}$ or $\varepsilon^{5/6}/k$, as in the case of the k-ω model,[13] although the predicted transformed velocity profiles in the log-law region are nearly exact.

IV. Compressibility Modifications

If one argues that the rise of the slope shown in Fig. 1 is mainly caused by the fact that compressibility terms arising from the averaging process were not taken into account, an alternative to changing the variables is to introduce additional compressibility-related model terms and/or to make the model coefficients depend on compressibility parameters. Because the rise of the slope indicates a reduction in eddy viscosity, corrections are needed to increase the turbulence energy level to increase the predicted value of the von Kármán constant κ. This requirement, however, is exactly opposite to that for mixing layer model corrections,[14,15] which call for a reduction of turbulence energy to accommodate the drop in spreading rate for high-Mach-number flows.

As most of the recent development of the compressibility model modifications has been centered on the prediction of mixing layers, it would be interesting to see how these modifications behave in a completely different situation, i.e., the boundary-layer flows. Four of the compressibility corrections which have produced good agreement with data in high-Mach-number mixing layers were examined in this study. The first two, by Sarkar et al.[14] (hereafter referred to as Sarkar 1) and Zeman[15] (Zeman 1), were based on the concept of dilatation dissipation, which assumes that the dissipation rate of turbulent kinetic energy contains two parts, the solenoidal (incompressible) and dilatational (compressible) parts, ε_s and ε_d, respectively.

$$\varepsilon = \varepsilon_s + \varepsilon_d \tag{24}$$

where ε_s is calculated from the incompressible form of the ε equation and ε_d is assumed to be a function of ε_s and turbulent Mach number M_t.

$$\varepsilon_d = F(M_t, \varepsilon_s) \approx F(M_t)\varepsilon_s \tag{25}$$

The function F and the turbulent Mach number M_t are defined as follows:

$$F = \alpha_1 M_t^2 \qquad \text{where } M_t = \frac{\sqrt{2k}}{c} \qquad \text{(Sarkar 1)}$$

$$F = c_d\left\{1 - \exp\left[-\left(\frac{(M_t - M_{to})\,H\,(M_t - M_{to})}{\sigma_M}\right)^2\right]\right\} \tag{26}$$

$$\text{where } M_t = \sqrt{\frac{1+\gamma}{2}}\,\frac{\sqrt{2k}}{c} \qquad \text{(Zeman 1)}$$

where c is the sound speed; H is the Heaviside unit step function; α_1, c_d, M_{to}, and σ_M are 1, 0.75, 0.1, and 0.6, respectively. Viegas and Rubesin[16] show that these compressibility modifications have improved the prediction of the mixing layer spreading rates.

The pressure dilatation correlation $\overline{p\partial u_i/\partial x_i}$ in the turbulent kinetic energy equation where u and p are fluctuating velocity and pressure, respectively, is the other focus in the modeling of the compressibility correction terms in the Couette-flow approximation;

$$-\frac{\mathrm{d}}{\mathrm{d}y}\left(\frac{\mu_t}{\sigma_k}\frac{\mathrm{d}k}{\mathrm{d}y}\right) = \rho P_k - \rho\varepsilon + \overline{p\partial u_i/\partial x_i} \tag{27}$$

Based on direct numerical simulation of isotropic turbulence and homogeneous shear flows, Sarkar et al.[17] (Sarkar 2) proposed the following model for the pressure dilatation:

$$\overline{p\partial u_i/\partial x_i} = -\alpha_2 \rho P_k M_t^2 + \alpha_3 \rho \varepsilon_s M_t^2 \tag{28}$$

where α_2 and α_3 are suggested to be 0.4 and 0.2, respectively. In addition, the value of α_1, shown in Eq. (26), is reduced to 0.5. Sarkar 2 has been tested successfully in predicting the spreading rate of high Mach number mixing layers.[18]

In an unpublished report from the University of Manchester Institute of Science and Technology (UMIST) group, El Baz[19] has proposed the following compressibility model corrections which can account reasonably well for compressibility effects in the mixing layers. First, the coefficient $c_{\varepsilon 2}$ is modified to include the Mach number effects:

$$c_{\varepsilon 2} = \frac{c_{\varepsilon 2}}{(1 + 3.2M_t^2)} \tag{29}$$

Second, the additional pressure-dilatation term is modeled as:

$$\overline{p\partial u_i/\partial x_i} = 3M_t^2\rho\left(\frac{4}{3}k\frac{\partial U_i}{\partial x_i} - P_k\right) \tag{30}$$

where the turbulent Mach number is defined as $M_t = \sqrt{k}/c$.

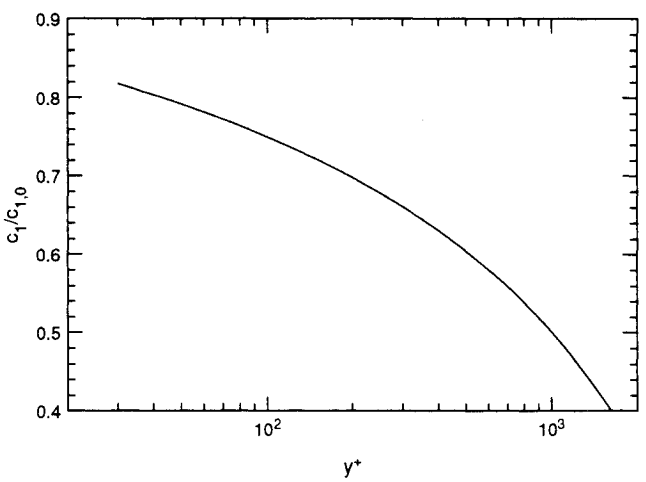

Fig. 5 Modified c_1 distribution of the k-ε model, M_τ = 0.12 and B_q = 0.

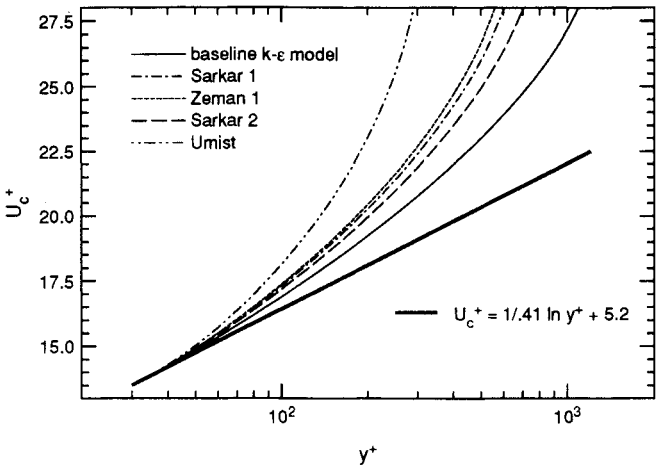

Fig. 6 Test of compressibility modifications in predicting compressible law of the wall.

The four model modifications, namely, Sarkar 1, Zeman 1, Sarkar 2, and Umist, were intended for the mixing layer. When applied to boundary layers, they tend to aggravate the model defects. In Fig. 6, the Couette flow solutions for $M_\tau = 0.12$ and $B_q = 0$ are presented. All model modifications yields even larger κ than the baseline model due to the reduction in turbulent energy level—an expected but undesirable outcome.

Two additional compressibility modifications, although not yet tested in mixing layers, are worthy of mention here. Rubesin[20] and Zeman[21] introduced an additional $\overline{p^2}$ equation, in which the pressure dilatation appears explicitly, representing the interchange of potential and kinetic energies. The $\overline{p^2}$ is derived from $\overline{\rho'^2}$, which is obtainable from the continuity equation. Rubesin assumed a polytropic process to relate ρ' to p whereas Zeman assumed an adiabatic process. In the log-law region, due to transport terms being negligible, the pressure dilatation can be expressed as

$$\overline{p\partial u_i/\partial x_i} = f(M_t)\left(\frac{d\rho}{dy}\right)^2 \frac{k}{\varepsilon}\frac{c^2}{\rho}\overline{v'^2} \tag{31}$$

where the function f is chosen as[21]

$$f = 0.2\left[1 - \exp\left(\frac{-M_t^2}{0.02}\right)\right] \tag{32}$$

Since Eq. (31) has a positive sign, it is expected to increase the turbulent energy level and hence reduce the value of κ for high-Mach-number flows. Huang[22] and Zeman[21] have independently tested the model and indeed found the modification improves the prediction of the log-law profiles, although its impact on the prediction of the mixing layer has yet to be tested. It should be noted that when convective transport of $\overline{p^2}$ is important, as in a wake or mixing layer, the simplified form of the pressure dilatation, shown in Eq. (31), is not readily available and further model assumptions are required to close the equations. These assumptions have introduced additional equations which make the final system of equations very stiff and difficult to solve. Viegas and Rubesin[16] have reported this problem in an attempt to solve the Rubesin model in the mixing layers.

V. Conclusions

The present study has shown that the extension of incompressible turbulence models to compressible flow requires density corrections to the closure coefficients to satisfy the law of the wall (logarithmic law in Van Driest transformed coordinates). The k-ω model appears to be more attractive than the k-ε model at high Mach numbers, because the coefficients of the unwanted density-gradient terms are smaller. A length-scale transport equation can be devised to minimize the density effects and has proved successful at least in boundary-layer flows.

Another interesting observation uncovered from this study is that current compressibility modifications, which were calibrated in the mixing layer, generally increase discrepancies between predictions and the Van Driest compressible law of the wall.

Finally, we emphasize again that although the above analysis was confined to two-equation models, our qualitative conclusions, and probably our selection of ω as the best of the current "dissipation" variables, should apply to Reynolds-stress transport models also.

References

[1]Rotta, J. C., "Turbulent Boundary Layers with Heat Transfer in Compressible Flow," AGARD Rept. 281, April 1960.

[2]Bradshaw, P., "Compressible Turbulent Shear Layers," *Annual Review of Fluid Mechanics*, Vol. 9, 1977, pp. 33–54.

[3]Fernholz, H. H., and Finley, P. J., "A Critical Commentary on Mean Flow Data for Two-Dimensional Compressible Turbulent Boundary Layers," AGARD-AG-253, May 1980.

[4]Huang, P. G., Bradshaw, P., and Coakley, T. J., "Skin Friction and Velocity Profile Family for Compressible Turbulent Boundary Layers," *AIAA Journal*, Vol. 31, No. 9, 1993, pp. 1600–1604.

[5]Coles, D., "The Turbulent Boundary Layer in a Compressible Fluid," Rand Corp., Rept. R-403-PR, Santa Monica, CA, Sept. 1962.

[6]Coakley, T. J., and Huang, P. G., "Turbulence Modeling for High Speed Flows," AIAA Paper 92-0436, Jan. 1992.

[7]Huang, P. G., and Coakley, T. J., "An Implicit Navier-Stokes Code for Turbulent Flow Modeling," AIAA Paper 92-0547, Jan. 1992.

[8]Huang, P. G., and Coakley, T. J., "Modeling Hypersonic Boundary-Layer Flows with Second-Moment Closure," *Near-Wall Turbulent Flows*, edited by R. M. C. So, C. G. Speziale, and B. E. Launder, Elsevier, Amsterdam, The Netherlands, 1993, pp. 199–208.

[9]Huang, P. G., and Coakley, T. J., "Calculations of Supersonic Flows Using Compressible Wall Functions," *Engineering Turbulence Modelling and Experiments*, edited by W. Rodi and F. Martelli, Elsevier, Amsterdam, The Netherlands, 1993, pp. 731–739.

[10]Gibson, M. M., and Launder, B. E., "Ground Effects on Pressure Fluctuation in the Atmospheric Boundary Layer," *Journal of Fluid Mechanics*, Vol. 86, Pt. 3, June 1978, pp. 491–511.

[11]Wilcox, D. C., "Reassessment of the Scale-Determining Equation for Advanced Turbulence Models," *AIAA Journal*, Vol. 26, No. 11, 1988, pp. 1299–1310.

[12]Wilcox, D. C., "Dilatation-Dissipation Corrections for Advanced Turbulence Models," *AIAA Journal*, Vol. 30, No. 11, 1992, pp. 2639–2646.

[13]Menter, F. R., "Influence of Freestream Values on k-ω Turbulence Model Predictions," *AIAA Journal*, Vol. 30, No. 6, 1992, pp. 1657–1659.

[14]Sarkar, S., Erlebacher, G., Hussaini, M. Y., and Kreiss, H. O., "The Analysis and Modeling of Dilatational Terms in Compressible Turbulence," *Journal of Fluid Mechanics*, Vol. 227, 1991, p. 473.

[15]Zeman, O., "Dilatation Dissipation: The Concept and Application in Modeling Compressible Mixing Layers," *Physics of Fluids A*, Vol. 2, No. 2, 1990, pp. 178–188.

[16]Viegas, J. R., and Rubesin, M. W., "A Comparative Study of Several Compressibility Corrections to Turbulence Models Applied to High-Speed Shear Layers," AIAA Paper 91-1783, June 1991.

[17]Sarkar, S., Erlebacher, G., and Hussaini, M. Y., "Compressible Homogeneous Shear: Simulation and Modeling," *Turbulent Shear Flows*, edited by F. Durst et al., Springer-Verlag, Berlin, 1992, pp. 249–267.

[18]Gatski, T. B., Sarkar, S., Speziale, C. G., "The Present State and Future Direction of Second Order Closure Models for Compressible Flows," Workshop on Engineering Turbulence Modeling, NASA CP-10088, Cleveland, OH, Aug. 21–22, 1991.

[19]El Baz, A. M., "Modelling Compressibility Effects on Free Turbulent Shear Flows," 5th Biennial Colloquium on Computational Fluid Dynamics, Internal Rept., Univ. of Manchester Inst. of Science and Technology, Manchester, England, UK, May 27, 28, 1992.

[20]Rubesin, M. W., "Extra Compressibility Terms for Favre-Averaged Two-Equation Models of Inhomogeneous Turbulent Flows," NASA CR-177556, June 1990.

[21]Zeman, O., "New Model for Super/Hypersonic Turbulent Boundary Layers," AIAA Paper 93-0897, Jan. 1993.

[22]Huang, P. G., "Comment on the Present State and the Future Direction of Second Order Closure Models for Compressible Flows," Workshop on Engineering Turbulence Modeling, NASA CP-10088, Cleveland, OH, Aug. 1991.